JOURNAL OF APPLIED POLYMER SCIENCE VOL. 18, PP. 1385–1396 (1974)

A Computer Simulation Study of the Low-Angle X-Ray Scattering Obtained from Triblock Copolymers

B. L. BROWN* and T. TAYLOR,† *Institute of Polymer Science, University of Akron, Ohio 44310*

Synopsis

Computer programs were developed to produce graphic plots which simulate the low-angle x-ray scattering curves obtained from cast films of triblock copolymers. Models were developed to take account of lattice paracrystallinity, a distribution in size of the scattering elements, various types of lattice packing, and the possibility of more than one type of lattice packing in a loosely bound paracrystal. These studies provide an insight into the possible structure of the macrolattices which have been observed with triblock copolymers.

INTRODUCTION

Recent studies[1–4] have shown that triblock copolymers of polystyrene–polybutadiene–polystyrene composition phase separate on being cast from solution producing a two-phase system consisting of regions of a high polystyrene content inset in a polybutadiene matrix. The formation of these polystyrene islands depends critically on the temperature and on the nature and rate of evaporation of the casting solvent. Further work[5,6] has shown that films cast from certain solvents may produce a regularly ordered three-dimensional array of the polystyrene endblocks in the polybutadiene matrix. This solid-state ordering which has been observed is reminiscent of the crystalline structures earlier reported with gels of triblock copolymers.[7,8] Evidently, the development of this ordered morphology is a function of the thermodynamics of the polymer solution,[9] and the kinetics of film deposition.[10]

Apart from cast samples, this phenomenon has also been observed in commercial samples[11] which have been molded and extruded. In this case, the mechanism of ordering would be by means of stress rather than from thermodynamic considerations.

As a consequence of this ordering, the peaks obtained from low-angle x-ray scattering studies cannot be explained as being due to a random

* Present address: School of Physical and Molecular Sciences, University College of N. Wales, Bangor, Caernarvonshire, N. Wales.

† Present address: Belden Corporation, Technical Research Centre, P.O. Box 386, Geneva, Illinois, 60134.

distribution of polystyrene spheres condensed in the polybutadiene matrix, as if from "frozen" liquid scattering, but must invoke for their explanation some concept of regularity which involves elucidation of the unit cell structure of the system.

In many inorganic crystals, a very high degree of ordering is achieved, which gives rise to very sharp x-ray scattering peaks, broadened only to a small extent, predominantly by thermal motion. The peaks observed in studies of these triblock copolymers are much less sharp. A model which appears particularly appropriate to these studies is that of the paracrystalline lattice introduced by Hoseman.[12,13] In this, successive translation vectors in the lattice vary statistically in length and direction, giving rise to broader reflections in the scattering pattern than would be expected from an ideal crystal.

The preliminary results reported here are from the computer simulation of low-angle x-ray scattering curves, as would be expected to be produced by spheres situated on a paracrystalline lattice. For comparison, curves have been generated corresponding to the scattering expected from randomly distributed spheres, according to the Zernike-Prins[14] equation, which accounts for interparticle interference.

Several models involving alternative conformations of spheres situated on lattices have been developed from the basic simulated structure. By consideration of these models, conclusions may be formulated which can assist in the interpretation of experimental data.

THEORETICAL BACKGROUND

The scattering from a regular *three-dimensional array of spheres* may be described by the convolution of a three-dimensional point array with that of a function describing the sphere scattering. In the case of unit cells containing more than one scattering element, a structure factor term must be included, giving a summation of the scattered intensities from the separate elements, this term providing the selection rules for scattering from the different lattice types. The scattering intensity is then described by the equation

$$I(S) = R^2(S) = G^2(S)Z^2(S)L^2(S) \tag{1}$$

where

$$G(S) = \left[\frac{4\pi a^3}{3}\right]\left[\frac{3\sin 2\pi \mathbf{aS} - 2\pi \mathbf{aS}\cos 2\pi \mathbf{aS}}{(2\pi a\mathbf{S})^3}\right] \tag{2}$$

$$Z(S) = \sum_{n=1}^{N} \exp\left[2\pi i(\mathbf{a}x_n + \mathbf{b}y_n + \mathbf{c}z_n)\mathbf{S}\right]$$

$$= \sum_{n=1}^{N} \exp\left[2\pi i(hx_n + ky_n + lz_n)\right] \tag{3}$$

$$L(S) = \frac{\sin(N_1\pi \mathbf{aS})}{\sin(\pi \mathbf{aS})} \cdot \frac{\sin(N_2\pi \mathbf{bS})}{\sin(\pi \mathbf{bS})} \cdot \frac{\sin(N_3\pi \mathbf{cS})}{\sin(\pi \mathbf{cS})}. \tag{4}$$

In these expressions, which are derived in more detail elsewhere,[19] $G(S)$, $Z(S)$, and $L(S)$ describe sphere scattering, structural interference, and lattice scattering, respectively, a is the sphere radius, $\mathbf{S}$ is the scattering vector, x_n, y_n, z_n are fractional unit cell coordinates, N is the number of scattering elements per unit cell, and h, k, l are reciprocal lattice indices.

Equation (4) represents a three-dimensional reciprocal lattice with maxima corresponding to $\mathbf{aS} = h$, $\mathbf{bS} = k$, and $\mathbf{cS} = 1$. N_1, N_2, and N_3 are the numbers of scattering points in each of three directions.

In a *paracrystalline lattice*, there will be a variation in displacements of the scattering centers from ideal lattice positions. If the displacements correspond to a Gaussian distribution, then we can write

$$I(S) = G^2(S)Z^2(S)\left\{\int_0^\infty \frac{\exp - (\mathbf{r}_p - \mathbf{r}_I^2)}{K} L(S)\right\}^2 d\mathbf{r} \tag{5}$$

K is twice the variance of the Gaussian distribution, $(\mathbf{r}_p - \mathbf{r}_I)$ represents the difference in position between a lattice vector in the paracrystalline lattice and that in the ideal lattice.

Scattering from *random spheres* has been treated by Guinier and Fournet.[14] For hard spheres Debye[15] obtained the expression

$$I(S) = G^2(S)\left\{1 - \frac{8V_0}{V_1} G(S)\right\}. \tag{6}$$

where V_0 and V_1 are the volume of, and available to each sphere, respectively.

Using the equations outlined here, computer programs were written to calculate values of the scattered intensities corresponding to random and ordered spheres.

COMPUTING CONSIDERATIONS

Computations of the theoretical x-ray scattering intensities were carried out using an I.B.M. 360 and later an I.B.M. 370 computer, the output being plotted graphically using a Calcomp plotter facility. All programs were written in FORTRAN IV.

The development of the scattering curves involved generation of sphere scattering intensities, then generation of expected lattice scattering intensities, which were modulated by the sphere scattering. Later modifications took account of paracrystallinity and structure factors.

The final expression for lattice scattering, eq. (1), represents the distribution of intensities in the three-dimensional reciprocal lattice.

Experimentally, the low-angle x-ray scattering spectrophotometer scans in one direction. However, if it is assumed that in a hypothetical sample all orientations of the scattering planes with respect to the incident beam are equally probable, then the observed intensity will be the resultant of folding onto one axis the resultants observed in traveling through the reciprocal lattice from the origin along all rows of reciprocal lattice points.

Owing to difficulties in computer storage access, it was not possible to use this physically realistic model, and hence the lattice plane separations were calculated from Bragg's law:

$$\frac{1}{d} = \sqrt{\frac{h^2}{\mathbf{a}^2} + \frac{k^2}{\mathbf{b}^2} + \frac{l^2}{\mathbf{c}^2}} \tag{7}$$

The calculated values of d were used in a one-dimensional function, giving in the case of an ideal lattice

$$R(S) = G(S)\frac{\sin N\pi dS}{\sin \pi dS}. \tag{8}$$

Values of d could thus be calculated for all required values of h, k, and l and lattice unit cell vectors **a, b,** and **c**.

The value of N corresponds to the number of scattered elements in an array, the width of the scattering intensity peaks being inversely proportional to the value of N. It would be expected that the value of N should vary statistically, but in these calculations it was necessary to keep the value of N constant because of computing time considerations. This leads to secondary maxima being observed at the sides of the main scattering peaks. In reality, with variation of N, these would not appear. In most of the computed output, a value of $N=40$ was used, corresponding to a lattice size of approximately 40,000 Å in all three directions. The actual value of N was considered to be unimportant, as the effects of small degrees of paracrystallinity produced appreciably greater broadening for all values of N above approximately 10.

In the expression

$$\mathbf{S} = \frac{2\sin\theta}{\lambda}$$

for low angle studies $\sin\theta \simeq \theta$. Curves were plotted up to a scattering angle of 2400 sec using this approximation.

In order to take account of the structure factors as required with the face-centered cubic type of packing, several 'IF' statements were written into the computer program such that only values of h, k, and l satisfying the structure factor equation produced theoretical scattering peaks.

The integrals were evaluated using Simpson's rule, by evaluation at 100 points throughout the ranges considered.

DISCUSSION

In order to produce a simulated computer scattering output representing experimentally obtained results, a sequence of scattering curves were developed.

The starting point for the computed models was the ideal simple cubic lattice of regular spheres. Figure 1 shows the sharp lattice scattering peaks modulated by the sphere scattering intensities as produced by this model. The scattering curves are consistent with a three-dimensional array having 40 elements in each direction.

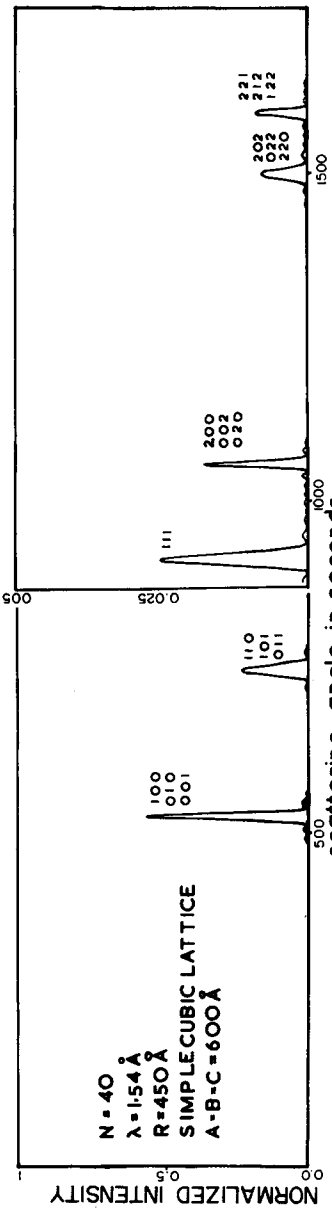

Fig. 1. Angular scattering intensity distribution expected for regular spheres situated on a regular single cubic (S.C.) lattice.

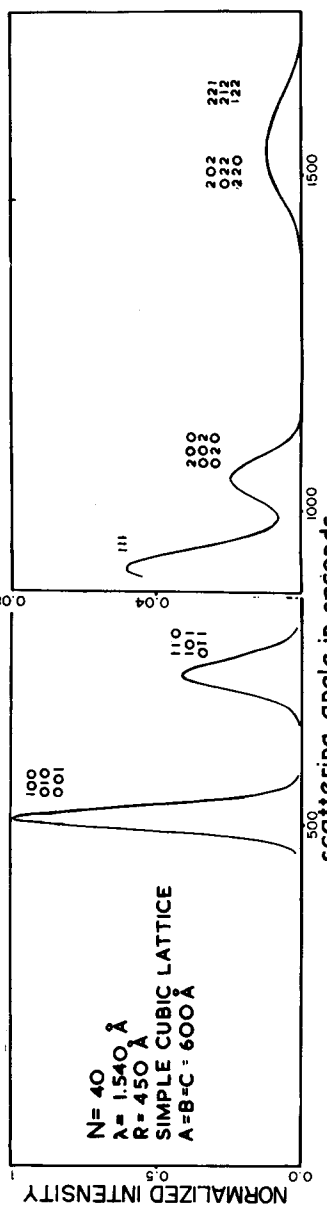

Fig. 2. Angular scattering intensity distribution expected for regular spheres situated on a paracrystalline S.C. lattice.

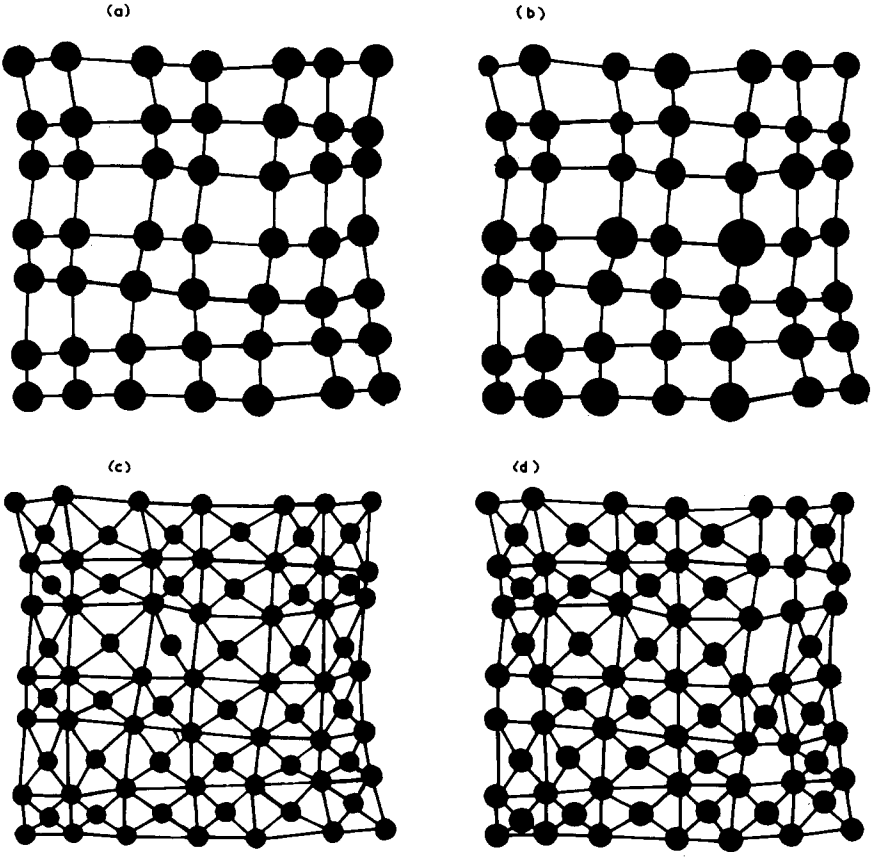

Fig. 3. (a) Two-dimensional projection of the lattice corresponding to Fig. 2 consisting of regular spheres situated on a paracrystalline S.C. lattice. (b) Two-dimensional projection of the lattice corresponding to Fig. 4 representing a distribution of sphere sizes situated on a paracrystalline S.C. lattice. (c) Two-dimensional projection representing regular spheres situated on a paracrystalline face-centered cubic (F.C.C.) lattice corresponding to Fig. 5. (d) Two-dimensional projection representing regular spheres situated on a paracrystalline F.C.C. lattice, containing small regions of S.C. character corresponding to Fig. 6.

A larger number of elements would sharpen the peaks still further, while a smaller number would produce the opposite result. As a consequence of not averaging statistically over different macrolattice sizes, secondary peaks are obtained at the sides of the main peaks. Consideration of eq. (8), shows that there are $(N - 2)$ secondary peaks between every two of the diffracted intensity peaks corresponding to a particular lattice separation.

The effect of paracrystallinity is to broaden the peaks as well as remove any secondary intensity maxima. Figure 2 shows the expected intensity distribution for a simple cubic lattice with a variance in the scattering vector lengths of 50 Å in 600 Å (67% of the scattering elements are within 50 Å of the mean position). Figure 3a shows the type of lattice which corresponds to this scattering. Noticeably the scattering peaks become

broader at higher scattering angles. Higher scattering angle peaks correspond to a narrowing in the separation of the scattering planes. As a result of paracrystallinity giving rise to a Gaussian distribution of scattering points about a mean, the effect on peak width broadening will be more prominent as the lattice plane separation diminishes. This is evident in Figure 2 by a comparison of the half-height peak widths for the (1,0,0), (0,1,0) and (0,0,1) peak with the (2,0,0), (0,2,0), and (0,0,2) peaks, these having half-height peak widths of approximately 40 Å and 70 Å, respectively.

Owing to the diffuse nature of the paracrystalline lattices, a variation in sphere size as well as a variation in lattice translation vectors is a possibility. With reference to eq. (2) and assuming a Gaussian distribution in sphere size about the mean, the resultant scattered intensity would be of the form

$$R(S) = \left[\int_0^\infty \exp - \frac{(a - a_0)^2}{K} G(S)da\right] Z(S)L(S) \tag{9}$$

where a_0 is the mean sphere radius and K is twice the variance in the sphere size distribution.

A model corresponding to this type of sphere scatterer distribution is shown in Figure 3b, whilst Figure 4 displays the expected intensity distribution, corresponding to a variance in the sphere size of 12%. Noticeably there is little difference in peak broadening with a distribution of sphere sizes; however, the relative heights of the peaks are altered. Physically this is to be expected, as the observed intensities are the resultant of the lattice scattering term multiplied by the sphere scattering term and the sphere scattering term is now changing more slowly than in Figure 2. Even if the sphere scattering intensity was to become extremely broad, corresponding to a very large variation in sphere size or to small spheres, it could only produce a resultant scattered intensity where the lattice scattering intensity was other than zero.

A face-centered cubic structure is very probable in any configuration involving close packing. Equation (3) shows that with a face-centered cubic structure, structure factor considerations eliminate scattering from planes other than those corresponding to $(h + k)$, $(k + l)$, and $(h + l) = 0$ or an even number. The first scattering peak observed thus corresponds to the (1,1,1) plane. For a given unit cell size, the peaks observed from face-centered lattice scattering are at higher angles than those obtained from simple lattice scattering. Figure 5 shows hypothetical curves for a paracrystalline F.C.C. structure with lattice unit cell dimensions double those of Figure 2. The curve corresponding to the (0,0,2), (0,2,0), and (2,0,0) planes in Figure 5 is now situated at the same position as the (0,0,1), (0,1,0), and (1,0,0) planes in the simple cubic case shown in Figure 2. For the F.C.C. lattice, however, the (1,1,1) peak appears adjacent to the (0,0,2), (0,2,0), and (2,0,0) peak. The influence of the degree of paracrystallinity on the separation of these two peaks gives some insight into the degree of paracrystallinity which may exist in real triblock copolymer lattices.

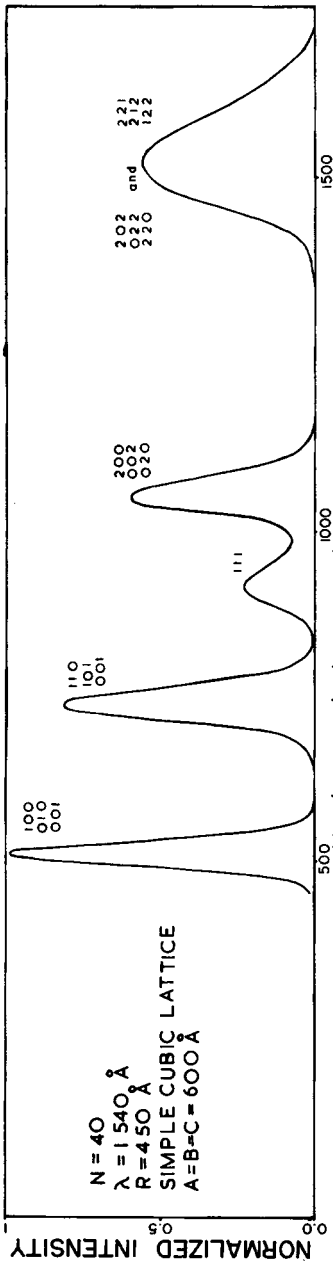

Fig. 4. Angular scattering intensity spectrum expected for a Gaussian distribution of sphere sizes situated on a paracrystalline lattice.

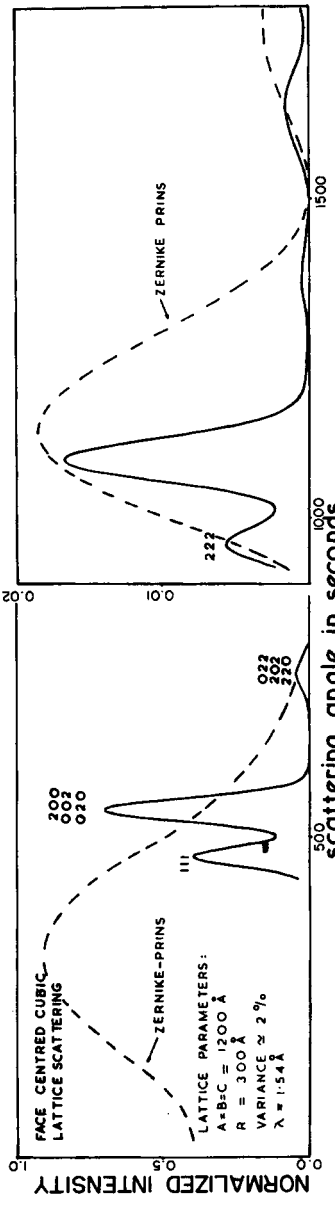

Fig. 5. Angular scattering intensity spectrum expected for regular spheres situated on a paracrystalline F.C.C. lattice. Broken line corresponds to the Zernike-Prins equation for a liquid consisting of regular spheres.

Thus, with a value of variance of 2% as shown in Figure 5, the two main peaks are separate. The fusing together of the two peaks as in Figure 6, for a value of variance of 4%, is indicative of the degree of paracrystallinity existing in real lattices, as in more than one experimentally reported study,[6,16] a first main peak of the shape shown in Figure 6 has been observed. It should not be forgotten that this type of double first main peak is suggestive of a F.C.C. lattice structure.

Also included in Figure 5 is a theoretically expected curve corresponding to eq. (15), with $V_0/V_1 = 0.1$. The broad nature of the theoretical peaks obtained with this equation provide further verification of ordering of the scattering regions in experimental samples, on comparison of the peak widths obtained.

An interesting phenomenon is indicated by the appearance of the peaks marked X and Y in Figure 6. In a loosely bound paracrystalline lattice of the type discussed here, it is possible that the lattice may not be completely simple cubic, as drawn in Figure 3a, or completely face-centered cubic, as suggested in Figure 3c. Rather, we may have predominantly one type of structure, probably face centered, but with small areas where the packing may be different. This is illustrated in Figure 3d, as a two-dimensional projection. Here, the packing is face-centered cubic, with 5% of simple cubic. A consequence of this would be a breakdown of the condition allowing only orders where $(h + k)$, $(k + l)$, and $(l + h) = 0$ or an even number to produce scattering.

Hence, in a predominantly face-centered cubic structure, a small amount of simple cubic structure will produce peaks corresponding to the (0,0,1), (0,1,0), (1,0,0), (1,1,0), (1,0,1), and (0,1,1) planes, these being degenerate to two peaks for a cubic type of structure. Figure 6 corresponds to scattering from a predominantly face-centered cubic structure containing 5% of simple cubic. The existence of small scattering peaks inside the first main scattering peaks has been reported.[6] Minor intensity peaks at this position would not be expected from a conventional Braggs' law analysis. One possible reason for the appearance of these peaks is that the phenomenon discussed above is occurring, namely, the macrolattices have predominantly face-centered cubic structure, but small regions of simple cubic structure are interdispersed such that complete extinction of the first few scattered intensity lines of the F.C.C. lattice does not occur.

Alternatively, the existence of these minor intensity peaks could be due to the regions of the macrolattices in the polymer all being of a well-characterized size, such that the value of N in eq. (4) is constant. The nature of the mathematical function $\sin N\theta/\sin\theta$, which is valid for an array of scatterers, would then produce $(N - 2)$ minor peaks inside the first main peak. The implication of this explanation would be that there is a thermodynamic reason for the macrolattice regions to grow to a discrete size; and although tantalizing, this prospect appears unlikely. More probably, the secondary peaks are produced as a result of imperfections in the loosely bound paracrystal. It is possible that in the instances where intensity

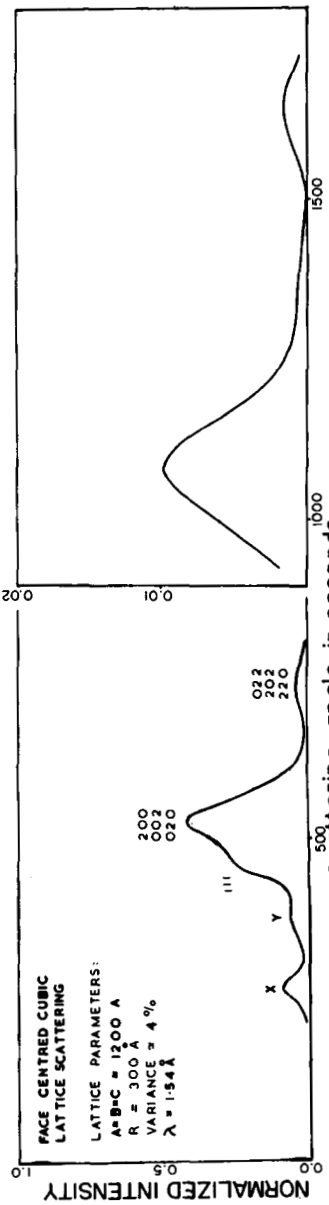

Fig. 6. Angular scattering intensity spectrum expected for regular spheres situated on a paracrystalline F.C.C. lattice with a small percentage of S.C. structure.

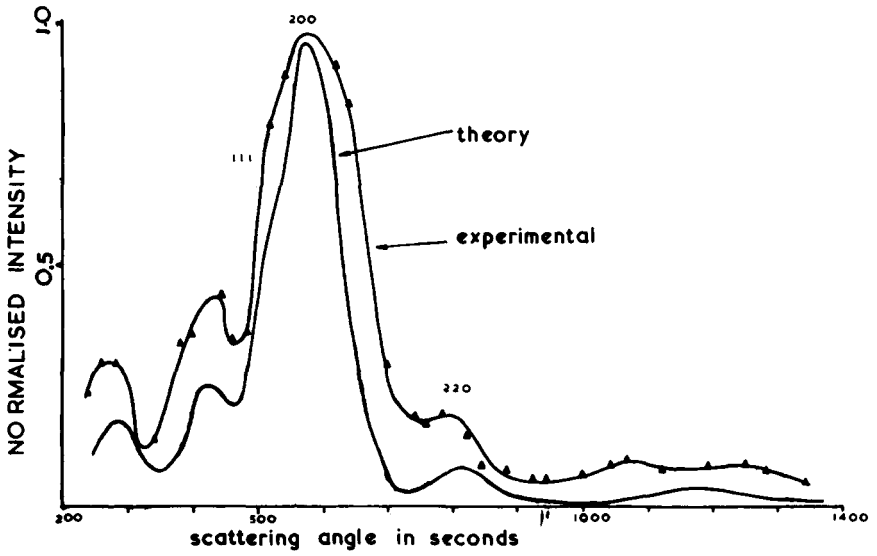

Fig. 7. Comparison of experimental curve obtained for S.B.S. (30% styrene) 950,000 molecular weight polymer with theoretical generated curve. The theoretical curve corresponds to a F.C.C. lattice of 1020 Å side, 4% paracrystallinity, and having 8% simple cubic structure in the polymer matrix.

peaks have been observed inside the main scattering peak, the type of slit correction used may have enhanced the relative intensities of the peaks obtained.[17,18]

Figure 7 shows an experimental curve fitted by the computer techniques described here for a cast film of S.B.S. copolymer of 950,000 molecular weight, demonstrating that it is possible to account both for the sample paracrystallinity and for possible faults in the lattice. Noticeably, this fitted curve demonstrates the high degree of ordering which may occur in these polymer systems: the 4% paracrystallinity corresponding to 66% of the scattering elements being within 41 Å of the mean lattice position.

Alternative structures to the one discussed here have been noted in triblock copolymers.[11,12] However, in cases where cylinders have been postulated as the configuration of the styrene portion of the triblocks, the direction of orientation of these cylinders is generally maintained constant over distances compatable to the size of the lattice. With samples of this type, scattering patterns will be obtained which vary with the orientation of the sample. Distinguishing between the scattering for randomly oriented close-packed bunches of cylinders and the systems reported here presents a more difficult problem, a study of which was not attempted in this work. Cylindrical systems have been investigated by several authors.[22–24] It is worth noting that owing to the different order of Bessel function operative in the scattering from cylinders as compared to spheres, single-particle intensity maxima occur at different angles for the same particle radius. Comparison of the ratios of scattering angles at which maxima are observed could provide a method for distinguishing between the two systems.

Qualitatively, the same information as described here is given by optical transformation techniques.[19,25] With a high-speed computer available, however, a much more flexible system is obtainable, obviating the necessity for cutting masks corresponding to the desired model system.

Other advantages of using a computer for this type of work are that the relative intensities are easily distinguished without recourse to photographic measuring techniques and three-dimensional models of polymer structure are readily acceptable.

The authors wish to thank the computing staff of the University of Akron for assistance with the writing of the programs for this work, in particular S. Sawan. We also thank Dr. Mc. Intyre for discussions of this work. One of us (B.L.B) thanks the N.R.C. for postdoctoral support during the tenure of which this work was performed.

References

1. J. F. Beecher, L. Marker, R. D. Bradford, and S. L. Aggarwai, *J. Polym. Sci. C*, **26**, 117 (1969).
2. M. Matsuo, *Jap. Plast.*, **2**, 6 (1968).
3. P. R. Lewis and C. Price, *Nature*, **223**, 494 (1969).
4. D. Mc. Intyre and E. Campos-Lopez, *Block Polymers*, Plenum Press, New York, 1970, pp. 19–30.
5. T. Inoue, M. Moritani, T. Hashimoto, and H. Kawai, *Macromolecules*, **4**, 4, 500 (1971).
6. D. Mc. Intyre and E. Campos-Lopez, *Macromolecules*, **3**, 322 (1970).
7. E, Franta, A. Skoulios, P. Rempp, and H. Benoit. *Makromol. Chem.*, **87**, 271 (1965).
8. P. Grosius, Y. Gallot, and A. Skoulios. *Makromol. Chem.*, **132**, 35 (1970).
9. U. Bianchi, E. Pedemonte, and A. Turturro. *Polym. Lett.*, **7**, 785 (1969).
10. T. Inoue, T. Soen, T. Hashimoto, and H. Kawai. *Macromolecules*, **3**, 87 (1970).
11. A. Keller, E. Pedemonte, and F. M. Willmouth, *Kolloid-Z. Z. Polym.*, **238**, 385 (1970).
12. R. Hoseman. *Z. Phys.*, **128**, 1, 464 (1950).
13. L. E. Alexander, *X-Ray Diffraction Methods in Polymer Science*, Wiley, New York, 1969, Chap. 7.
14. A. Guinier and G. Fournet, *Small-Angle Scattering of X-Rays*, Wiley, New York, 1955.
15. P. Debye, *Z. Phys.*, **28**, 135 (1927).
16. L. J. Fetters, B. H. Meyer, and D. Mc. Intyre, *J. Appl. Polym. Sci.*, **16**, 1873 (1972).
17. P. Schmidt, *Acta Cryst.*, **19**, 938 (1965).
18. E. Campos-Lopez, D. Mc. Intyre, and L. J. Fetters, *Macromolecules*, **6**, 415 (1973).
19. H. Lipson and C. A. Taylor, *Fourier Transforms and X-Ray Diffraction*, Bell, London, 1958.
20. S. G. Lipson and H. Lipson, *Optical Physics*, Cambridge University Press, Cambridge, 1969.
21. C. Price, A. G. Watson, and M. T. Chow, *Polymer*, **13**, 333 (1972).
22. G. Oster and D. P. Riley, *Acta Cryst.*, **5**, 272 (1952).
23. R. E. Burge, *Acta Cryst.*, **12**, 285 (1959).
24. R. E. Burge, *Proc. Roy. Soc.*, **A260**, 558 (1961).
25. H. Lipson, *Optical Transforms*, Academic Press, New York, 1972.

Received April 14, 1973
Revised October 5, 1973